Available online at www.sciencedirect.com

ScienceDirect

Procedia CIRP 108 (2022) 194–198

www.elsevier.com/locate/procedia

6th CIRP Conference on Surface Integrity

Hardness Penetration Depth Prediction in the Grind-Hardening Process through a Combined FEM model

Flavia Lerra[a], Alessandro Ascari[a], Alessandro Fortunato[a]*

[a] *University of Bologna, Viale Risorgimento 2, 40136 Bologna, Italy*

* Corresponding author. Tel.: +39 051 2093456; *E-mail address:* alessandro.fortunato@unibo.it

Abstract

The grind-hardening process aims to increase the surface hardness of the material through the dual action of the mechanical and thermal load. A novel approach to model the process and predict the hardness penetration depth was developed based exclusively on the prediction of austenite-martensite transformation. A combined micro and macro scale approach was implemented to forecast the temperature reached in the surface starting from the action of a single grain and using its specific cutting power to design a moving heat source representing the interaction between the grinding wheel and the material. The martensitic transformation temperature considered in this paper takes into consideration the fast heat cycle typical of this process. In order to validate the model, tangential surface grinding tests were performed on 42CrMo4 and microstructural analysis with micro-hardness measurements were performed. This research presents a first step in developing a grinding process simulation that includes multi-grain grinding, real grain geometries, binder effect, and real workpiece-grinding wheel kinematics.

Keywords: Grind-hardening; FEM simulation; surface hardening; hardness penetration depth

1. Introduction

In the current manufacturing practice, mechanical components which are used in high load and sliding contact applications need to be heat treated to achieve specific hardness requirements on the working surface. In general, the components after a soft machining must be transported to the heat treatment facility and then introduced again into the production line for the final finishing phase. Brinksmeier et al. introduced for the first time the grind-hardening technology as an alternative to the current manufacturing route [1,2], in order to avoid the logistic and economic difficulties in integrating the heat treatment into the production chain. Moreover, this technology completely embodies the process integration and green manufacturing engineering target in the industry sector. Grind-hardening adopting higher depth of cut and applied on highly quenchable material could be considered an available surface modification technology. It exploits the mechanical and thermal load combination to induce a martensitic transformation and increase the surface hardness of the components without the intermediate heat treatment phase. Many researchers have focused on the experimental evaluation of the grind-hardening process [3-7] and a number of models focused on temperature field generated in the material taking into consideration the hardness penetration depth in the workpiece [8-11]. In this paper a novel approach to simulate the formation of the hardened depth in the grind-hardening process was proposed avoiding expensive and time-consuming experimental measurements. The model is developed in two hierarchical steps: the first step is a micro scale mechanical

10.1016/j.procir.2022.03.034

model where the action of a single grain was investigated with the aim at calculating the single grain cutting force and power generated; the second step is a macro scale thermal model where the interaction between the whole grinding wheel and the workpiece was considered as a moving heat source developed starting from the single grain cutting power and the wheel specification. With this approach, multi grains grinding can be simulated, together with the effects of the binder on process, and real wheel-workpiece kinematics can be easily taken into consideration [12]. Moreover, in the proposed model, transition temperatures martensite-austenite takes into account fast and not uniform heat cycles which lead to temperature transformation very far from conventional microstructural transformations in steel (quenching and tempering) [13]. To the best of the authors' knowledge, none of these elements have been addressed in the literature [14]. Single grain grinding tests and simulations were validated based on forces measurements previously. For this research a thermal model was developed, and tangential grinding tests were performed adopting high depth of cut able to reach the grind-hardening target. The thermal model allowed to calculate the temperature field in the workpiece after the wheel pass giving an indication of the hardness values reached in the contact zone. Microstructural analysis using an optical microscope with microhardness measurements were performed to verify the effect of the process on the material and validate the model.

2. Model description

A hierarchical FEM model was developed to predict the thermal effect of grind-hardening with the aim at forecasting the hardness penetration depth in the material surface. At first a single grain grinding model was developed in DEFORM 3D software to represent the mechanical interaction of a single abrasive with the material from a micro-scale point of view. Detailed explanation of the single grain griding model validation and development was reported in [12] and outline is presented in Fig.1. Power calculated during the contact of a single grain with the material considers all the contributions generated by the grinding action, rubbing, plowing and cutting phase. A specific power *Psp* value was considered such as the ratio between the power value reached during the pass and the total cut area generated. Power data obtained were introduced in the thermal model developed in COMSOL MULTIPHYSICS to create the heat source representing the grinding wheel pass. The action of the grinding wheel on the workpiece was replaced with a moving heat source with a translational speed equal to the feed rate value adopted during the tangential grinding tests and a constant heat flux value distributed in the contact area directly derived from the single grain specific power calculation. The power per grain *P* defined for the heat source entity was calculated by multiplying the specific grinding power *Psp* with the grain–workpiece contact area calculated as the frontal contact area of a sphere having dimensions corresponding to the nominal abrasive grain size with the workpiece surface at the chosen depth of cut [15]. Moreover, it was multiplying with the average number of grains per mm^2 which was approximated considering the properties of the wheel used for model validation. The simulation plan was developed with the same process parameters according to the single grain grinding model and

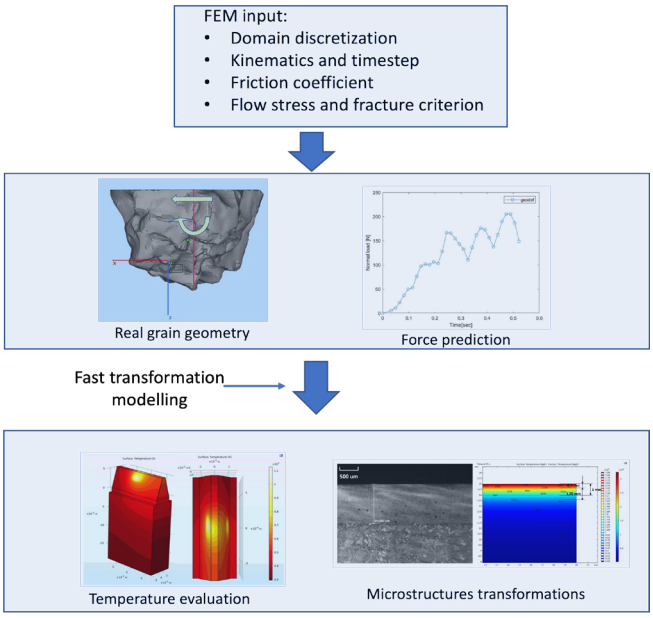

Fig. 1. Schematic description of the termo-mechanical model used

Table 1. Martensite and austenite thermal conductivity varying with the temperature.

T [°C]	0	300	600	800
Austenite thermal conductivity k [W/m K]	15	18	21.7	25.1
Martensite thermal conductivity k [W/m K]	43.1	36.7	30.1	

A simulation plan varying the depth of cut (p = 100 - 200 - 300 µm) and feed rate values (v_{ft} = 10 - 20 - 40 mm/s) was developed using a fixed value of cutting speed (v_c = 20 m/s). Model validation was provided by performing microstructural analysis and micro-hardness measurements towards the cross section of the material and comparing them with the calculated temperature field. To define the effective phase transformation transition threshold temperature was identified. Since the dry grinding process could be assimilated to a fast-heating thermal cycle, the critical temperature of the martensite to austenite transformation is slightly different compared to the austenitization temperature.

In order to determine initial and final temperatures of microstructural transformations in steel under severe thermal cycles, a Gleeble 3180 physical simulator were used in cylindrical specimen. Gleeble test can rapidly heat and cool the tested samples, allowing for the measurement of thermal expansions caused solely by microstructural transformations, as well as the recording of the temperatures at which these expansions / transformations take place.

The output given by the Gleeble is the dilation-temperature behavior of the specimen subjected to the abovementioned thermal cycle. For a better understanding, we present in Fig 2 the outcomes of heating a previously hardened specimen, where the temperatures at the start and end of tempering (395 °C and 520 °C respectively), as well as the start of

reaustenitization (712 °C), are shown. As a consequence, in this paper, 712°C is assumed as the threshold temperature for tempered martensite transformation into austenite. More explanations are reported in [14].

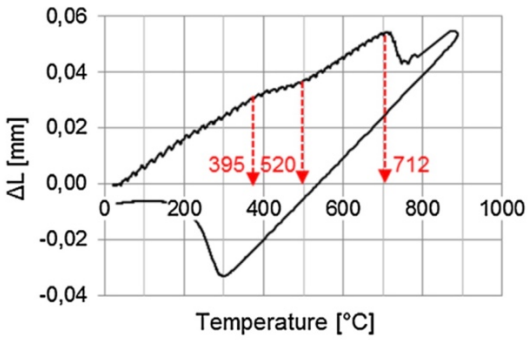

Fig. 2. Experimentally evaluated transformation temperatures for a fully hardened steel under fast heat cycles [14]

3. Experimental procedure

Grinding tests were performed on a CN Linea Iron 06.3 tangential grinding machine using a sintered aluminum oxide grinding wheel with a diameter of 280 mm and a width of 50 mm. The experimental plan was performed in dry conditions using the process parameters adopted reported in Table 2.

Table 2. Tangential grinding tests process parameters

v_c [m/s]	v_{ft} [mm/s]	a_e [mm]	Grinding mode
20	10	0,1	Up-grinding
	20	0,2	
	40	0,3	

The wheel grains FEPA size was equal to 60 with an average diameter equal to 0.25 mm. The thermal model adopted a griding heat source directly dependent to the number of grains exposed on the wheel surface, so that, it was considered a uniform distribution of the grains, with a percentage of active grain approximated to 80% compared to the theoretical total number of grains in a mm^2. Therefore, a grain area density of 13 grain/mm^2 was introduced in the model. Prismatic 42CrMo4 steel workpiece with dimension 20x15x15 mm was adopted for the experiments. Sample blocks were previously laser hardened to reach a hardness of 750 HV1 in the surface layer up to 1 mm of depth. Each sample was ground with a total depth of cut of 0,1 mm every 3 µm before each grinding test to guarantee the surface planarity. A grinding wheel dressing was performed before each experiment. Microstructural analysis and micro-hardness measurements were provided to verify the effect of the grinding process on the samples and validate the model. Microstructural analysis was carried out with an optical microscope Zeiss Axio Vert.A1M on the samples prepared according to standard metallographic techniques comprising mechanical grinding (80-2400 grit paper) and polishing with alumina in suspension down to a particle size of 1 µm. To reveal microstructural features, the samples were etched using Nital reagent for 3 s. Vickers micro-hardness tests were performed using a load of 1000 g for 20 s towards the hardened depth with indents spaced of 100 µm.

4. Results and discussion

This work aimed to define a suitable model to predict the hardness penetration depth in the grind-hardening process with the scope to avoid time-consuming experimental tests for the process power identification. It allows to represent the grinding wheel pass on the material as a moving heat source starting directly from the calculation of the single grain grinding power and the wheel grain dimension. In Fig. 3-5, the hardened depth obtained with a constant feed rate, respectively equal to 10 mm/s and the depth of cut of 100, 200 and 300 µm was compared with the temperature field calculated trough the proposed model. Good agreement was shown between the hardness thickness values detected by means the microstructural analysis and the temperatures calculated at the sample surface. The hardened depth thickness increases with the grinding depth of cut due to the increase of the thermal power absorbed by the material.

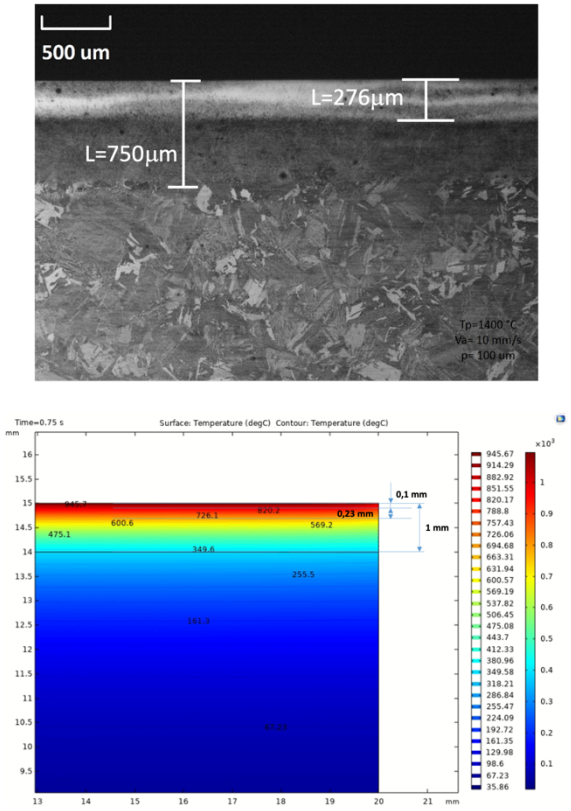

Fig. 3. Comparison between the microstructural analysis and the calculated temperature field with v_{ft} = 10 mm/s and a_e = 100 µm

In Fig. 6 the micro-hardness measurements were reported to show the penetration depth values obtained by grinding 100, 200 and 300 µm with a feed rate of 10 mm/s. Fig. 7 shows a resume of the comparison between the hardness penetration depth values revealed by the microstructural analysis and the hardened depth valued calculated by means of the described thermal model applying a feed rate of 10, 20 and 40 mm/s and a depth of cut of 100, 200 and 300 µm. A maximum percentage difference of 14% was reported between experimental tests and the model outcomes.

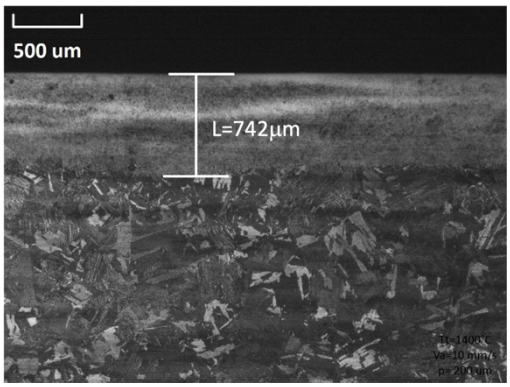

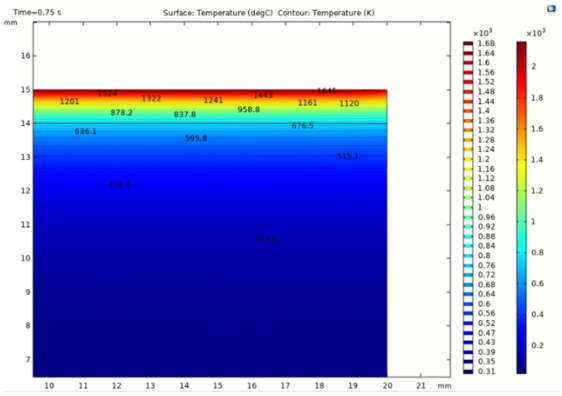

Fig. 4. Comparison between the microstructural analysis and the calculated temperature field with v_{ft} = 10 mm/s and a_e = 200 µm

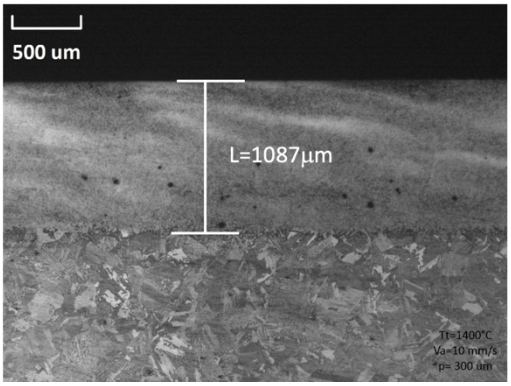

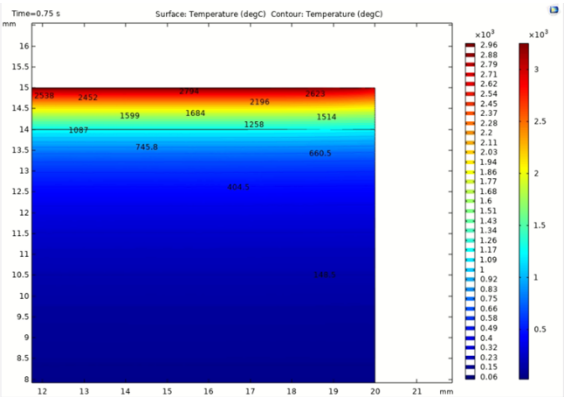

Fig. 5. Comparison between the microstructural analysis and the calculated temperature field with v_{ft} = 10 mm/s and a_e = 300 µm

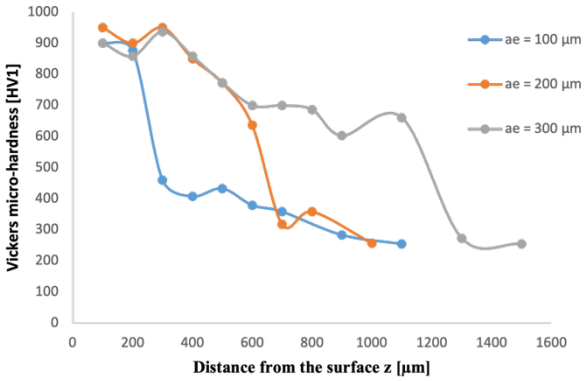

Fig. 6. Micro-hardness measurements with v_{ft} = 10 mm/s and a_e = 100, 200 and 300 µm

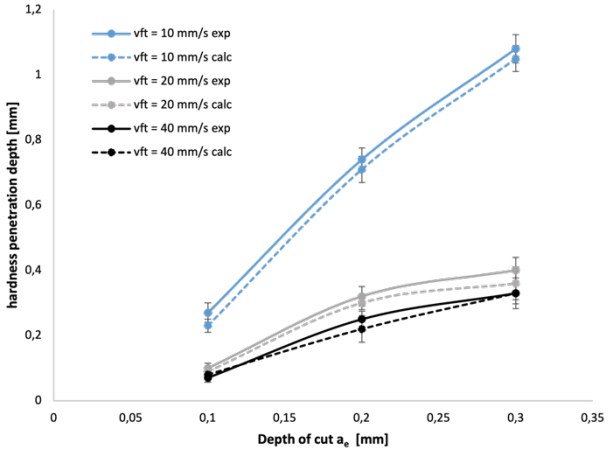

Fig. 7. Experimental and calculated hardness penetration depth comparison

5. Conclusions

In this paper a novel approach to simulate the formation of the hardened depth in the grind-hardening process was proposed avoiding expensive and time-consuming experimental measurements. The model was developed in two hierarchical steps. The first step is a micro scale mechanical model where the action of a single grain was investigated with the aim at calculating di specific cutting power generated. For the second step, a thermal model was developed, and tangential grinding tests were performed adopting high depth of cut able to reach the grind-hardening target. The thermal model allowed to calculate the temperature field in the workpiece after the wheel pass giving an indication of the hardness values reached in the contact zone. The model was validated through microstructural analysis and microhardness measurements to verify the effect of the process on the material and validate the model. Good agreement with a maximum percentage error of 14 % was achieved by comparing the hardness penetration depth thickness calculated with the model and experimentally detected. This research presents a first step in developing a grinding process simulation that includes multi-grain grinding, real grain geometries, binder effect, and real workpiece-grinding wheel kinematics.

Acknowledgement

This work is under the framework of EU Project FATECO. This project has received funding within the financial aid call of Research Fund Coal and Steel (RFCS-2018), with 847284 references. The dissemination results herein reflect only the author's view and the Commission is not responsible for any use that may be made of the information it contains.

References

[1] E. Brinksmeier and T. Brockhoff, "Utilization of Grinding Heat as a New Heat Treatment Process," *CIRP Ann. - Manuf. Technol.*, vol. 45, no. 1, pp. 283–286, 1996, doi: 10.1016/S0007-8506(07)63064-9.

[2] T. Brockhoff and E. Brinksmeier, "Grind-hardening: a comprehensive view," *CIRP Ann. - Manuf. Technol.*, vol. 48, no. 1, pp. 255–260, 1999, doi: 10.1016/S0007-8506(07)63178-3.

[3] I. Zarudi and L. C. Zhang, "Mechanical property improvement of quenchable steel by grinding," *J. Mater. Sci.*, vol. 37, no. 18, pp. 3935–3943, 2002, doi: 10.1023/A:1019671926384.

[4] J. D. Liu, J. Z. Zhuang, and S. W. Huang, "Influence of the grinding pass on microstructure and its uniformity of the grind-hardened layer," *Adv. Mater. Res.*, vol. 211–212, pp. 36–39, 2011, doi: 10.4028/www.scientific.net/AMR.211-212.36.

[5] J. Liu, W. Yuan, S. Huang, and Z. Xu, "Experimental Study on Grinding-hardening of 1060 Steel," *Energy Procedia*, vol. 16, pp. 103–108, 2012, doi: 10.1016/j.egypro.2012.01.019.

[6] M. Liu, T. Nguyen, L. Zhang, Q. Wu, and D. Sun, "Effect of grinding-induced cyclic heating on the hardened layer generation in the plunge grinding of a cylindrical component," *Int. J. Mach. Tools Manuf.*, vol. 89, pp. 55–63, 2015, doi: 10.1016/j.ijmachtools.2014.11.003.

[7] D. Hou, S. Gao, J. Liu, and S. Huang, "Effect of Grinding Parameters on the Hardness Penetration Depth of the Steel GCr15 in Internal Grind Hardening Process," *J. Phys. Conf. Ser.*, vol. 1637, no. 1, 2020, doi: 10.1088/1742-6596/1637/1/012112.

[8] M. Liu, K. Zhang, and S. Xiu, "Mechanism investigation of hardening layer hardness uniformity based on grind-hardening process," *Int. J. Adv. Manuf. Technol.*, vol. 88, no. 9–12, pp. 3185–3194, 2017, doi: 10.1007/s00170-016-9029-y.

[9] Y. Guo, S. Xiu, M. Liu, and X. Shi, "Uniformity mechanism investigation of hardness penetration depth during grind-hardening process," *Int. J. Adv. Manuf. Technol.*, vol. 89, no. 5–8, pp. 2001–2010, 2017, doi: 10.1007/s00170-016-9234-8.

[10] X. Zhang, S. Xiu, and X. Shi, "Study on the distribution of hardening layer of 40Cr and 45 steel workpiece in grind-hardening process based on simulation and experiment," *Int. J. Adv. Manuf. Technol.*, vol. 93, no. 9–12, pp. 4265–4283, 2017, doi: 10.1007/s00170-017-0819-7.

[11] A. Rajaei, B. Hallstedt, C. Broeckmann, S. Barth, D. Trauth, and T. Bergs, "Numerical Prediction of the Microstructure and Stress Evolution During Surface Grinding of AISI 52100 (DIN 100Cr6)," *Integr. Mater. Manuf. Innov.*, vol. 7, no. 4, pp. 202–213, 2018, doi: 10.1007/s40192-018-0122-y.

[12] F. Lerra, E. Liverani, E. Landi, and A. Fortunato, "Real single grain grinding FEM simulation for case-hardened steel based on equivalent contact area analysis," *J. Manuf. Sci. Eng.*, pp. 1–24, 2021, doi: 10.1115/1.4051536.

[13] E. Liverani, D. Sorgente, A. Ascari, L. D. Scintilla, G. Palumbo, and A. Fortunato, "Development of a model for the simulation of laser surface heat treatments with use of a physical simulator," *J. Manuf. Process.*, vol. 26, pp. 262–268, 2017, doi: 10.1016/j.jmapro.2017.02.023.

[14] S. Malkin, C. Guo, "Thermal Analysis of Grinding" Annals of CIRP, vol 56 (2): 760-782, 2007, doi: 10.1016/j.cirp.2007.10.005

[15] G. Guerrini, A. H. A. Lutey, S. N. Melkote, A. Ascari, and A. Fortunato, "Dry generating gear grinding: Hierarchical two-step finite element model for process optimization," *J. Manuf. Sci. Eng. Trans. ASME*, vol. 141, no. 6, pp. 1–9, 2019, doi: 10.1115/1.4043309.

[16] A. Sue and G. Schajer, *Material Factors - Handbook of residual stressand deformation of steel*. 2002.